

Microwave liquid crystal wavelength selector

Fuzi Yang and J. R. Sambles^{a)}

Thin Film Photonics Group, School of Physics, University of Exeter, Exeter, EX4 4QL, United Kingdom

(Received 18 July 2001; accepted for publication 10 September 2001)

The combined use of a zero-order grating with liquid crystals to control microwaves is presented. A nematic liquid crystal is aligned in the $75\ \mu\text{m}$ gaps of a grating comprised of 1-mm-thick aluminum slats. A set of resonant transmission frequencies is recorded for microwaves incident on this structure with their electric field perpendicular to the slats. These resonances are due to the excitation of coupled surface plasmons. A voltage applied between adjacent pairs of slats causes the liquid crystal to realign, allowing sensitive control of the transmitted microwave frequencies. © 2001 American Institute of Physics. [DOI: 10.1063/1.1419240]

It has long been established that many thermotropic liquid crystals (LC) have a high optical birefringence. While this has been used extensively in low voltage driven liquid crystal displays it has yet to be significantly exploited with microwaves even though the birefringence extends into this frequency range.¹ A few microwave modulation devices involving waveguide¹⁻³ or microstrip-line⁴ structures which use the large dielectric anisotropy of LC materials have been reported. However, possibly through a perceived lack of suitable geometries for use of thin films of liquid crystal in the microwave wavelength range, few practicable devices have been developed.

Recently, however, a range of experiments and theoretical models have been presented which show strongly enhanced transmission of electromagnetic radiation through thin, periodic metallic samples containing very small hole arrays⁵⁻⁷ or thicker samples having narrow slits.^{8,9} Both have been attributed to⁸ the resonant coupling of surface plasmon polaritons (SPPs) causing the transmission of radiation through structures with dimensions much less than the radiation wavelength. For narrow slit structures, with the sides of the grooves very close together, the evanescent fields of excited SPPs on each side of a single groove interact. Then, for certain groove depths, the SPPs set up coupled standing waves resulting in field enhancements within the grooves^{10,11} and strong transmission. If, in addition, the pitch of the grating is shorter than half of the incident wavelength, the grating is zero order acting simply as a selective reflector or transmitter of the incident radiation. This selective resonant transmission phenomenon through deep narrow grooves in metallic structures has now been reported at microwave frequencies.¹²

In this letter, we present results of voltage controlled wavelength selection at microwave frequencies by use of metallic slat gratings with the thin grooves between the metallic slats filled with liquid crystal. As shown in Fig. 1, a very deep zero-order metallic grating is built by stacking 55 strips of aluminum with mylar spacers at each end. The dimensions of the slats are length $L = 60.0\ \text{mm}$, width (groove depth) $W = 30.0\ \text{mm}$, and thickness $D_{\text{Al}} = 1.0\ \text{mm}$. The crucial thickness of the mylar-spaced gaps is only D_{LC}

$= 75.0\ \mu\text{m}$. The depth-to-pitch ratio of the gratings is about 30:1. They are zero order for wavelengths above about 2 mm and the thin gaps may be readily filled with a relatively small amount of liquid crystal. To facilitate alignment of the liquid crystal, the slats are individually coated with a polyimide (AL 1254) film on both sides. They are then baked and unidirectionally rubbed along the short axis direction of the slats to provide homogeneous alignment of the liquid crystal molecules. The polyimide layers also act as ion barriers preventing ions entering the thin liquid crystal layers when a field is applied. These coated aluminum slats are then stacked as the above array and capillary filled with a nematic liquid crystal (Merck-E7). Alternate slats are connected to an ac voltage source (1 kHz) allowing the application of the same voltage across every gap as shown in Fig. 1. This deep zero-order grating structure is now examined for its microwave transmittance properties.

The experimental apparatus is organized as shown in Fig. 2. A horn antenna, fed by a variable frequency microwave generator (26.0–40.0 GHz), is set a little beyond the focal point of a concave mirror with focal length about 2.0 m. This provides a weakly focusing beam directed at the grating sample, placed just in front of the final focus, which is at the detector horn. The zero-order transmitted beam is collected by the horn antenna of the detector, which is connected to a scalar network analyzer. Because the grating is quite close to the detector horn the grating sample is rotated

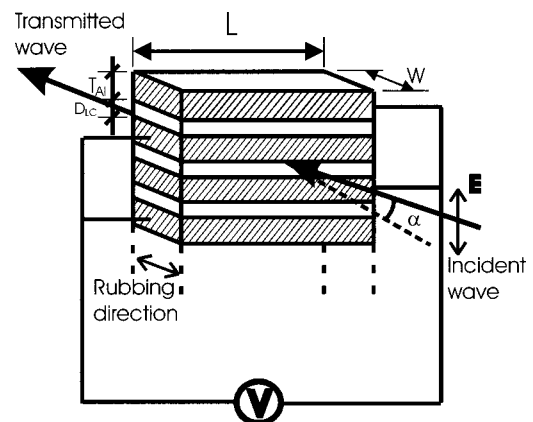


FIG. 1. Sample geometry.

^{a)}Electronic mail: j.r.sambles@exeter.ac.uk

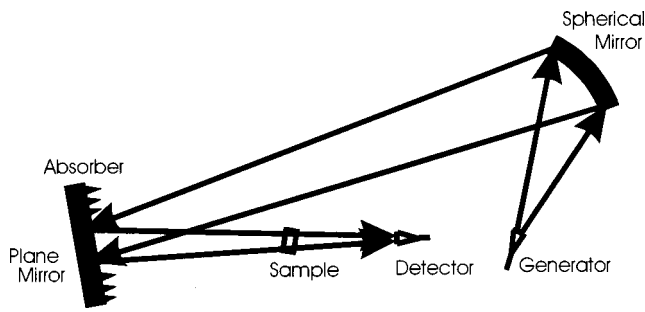


FIG. 2. Experimental setup.

so that the incidence angle is $\sim 20.0^\circ$. This avoids strong interference between the back surface of the grating and the detector horn. Only linearly polarized microwaves are incident with the electric vector lying perpendicular to the groove direction as shown in Fig. 1. As expected, no transmission is obtained for radiation polarized along the slit direction. Transmission data are taken as a function of frequency and also of applied voltage across the liquid crystal filled gaps. Figure 3 shows the frequency- and voltage-dependent transmissivity for the sample with voltage varying from 0.0 to 7.0 V. In Fig. 3 the curves from the bottom to the top are the response for the voltages: 0.0, 1.0, 1.2, 1.4, 1.5, 1.6, 1.8, 2.0, 3.0, 4.0, 5.0, 6.0, and 7.0 V, respectively. These data have been normalized with respect to the signal obtained in the absence of the slat sample.

There is a set of resonant transmission peaks. Their frequencies, at least at zero volts, are readily calculated from a simple model. As a consequence of the high conductivity of the aluminum, the fields of the SPP excited on the slat surfaces in the grooves are excluded from the metal, thus there is no coupling between fields in neighboring grooves and the fields are concentrated within the cavities. In addition, because aluminum at microwave frequencies has a permittivity with a very large real part ($\sim -10^5$) and there are narrow gaps (about $75 \mu\text{m}$) the coupled SPPs will have a wave vector very close to the wave vector in the dielectric filling the gaps.¹¹ Therefore, the coupled SPPs will be resonantly excited when the free space wavelength of the microwave radiation, λ_0 , satisfies¹³ $\lambda_0 = 2nW \cos \alpha/N$, where N is the

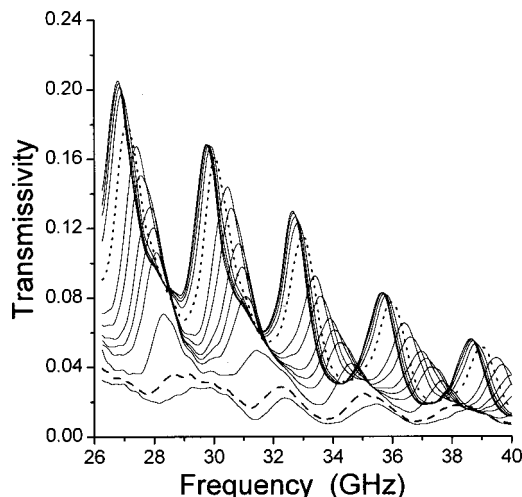


FIG. 3. Transmission data as a function of frequency and applied voltage for microwaves polarized perpendicular to the grating slats.

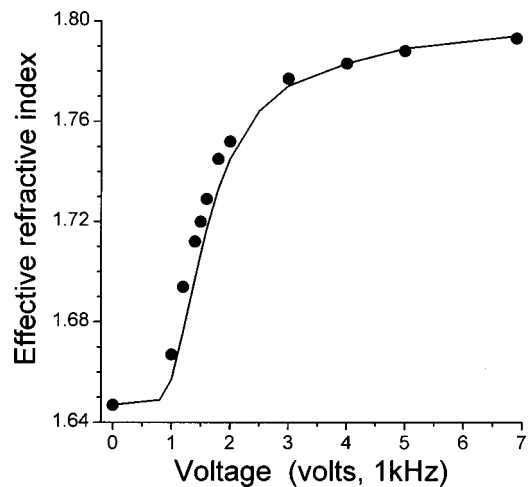


FIG. 4. Variation of the effective index as a function of the applied voltage.

number of nodes (regions of zero fields), n is the refractive index for the wavelength within the cavity, and α is the incident angle, $\sim 20.0^\circ$, of the radiation. Thus this type of sample, for which there is no diffraction, can be described as a pseudo, or “metal-filled” Fabry-Pérot interferometer, the two highly reflecting surfaces being the front and back surfaces of the aluminum slats.¹² The Fabry-Pérot nature of the resonant transmissivity is apparent from Fig. 3.

It is also apparent that one mode step in frequency is encompassed by changing the voltage from 0.0 to 7.0 V. The most rapid movement of the modes occurs between 1.0 V (dashed curve in Fig. 3) and 3.0 V (dotted curve in Fig. 3). The mode order numbers from high to low frequency are calculated as $N=13, 12, 11, 10$, and 9, respectively. In addition, the effective refractive index as a function of voltage may be obtained as shown in Fig. 4 as solid circles. From Fig. 4 we see a fast change of index with voltage between 1.0 and 3.0 V, after which it appears to saturate. This is simply because at these voltages the LC director is almost completely homeotropically aligned throughout each cavity. From this we deduce that the index obtained at 7.0 V, $n = 1.793$, is effectively the extraordinary index of the E7, n_e , for this frequency region. This accords well with the result of Lim.² Fitting data at zero field gives $n = 1.647$ which lies between $n_r = 1.664$, the average randomly aligned refractive index measured by Lim,² and $n_o = 1.598$, the ordinary index calculated by Lim² from n_e and n_r . This may mean that the LC director is only partially homogeneously aligned by the rubbed polyimide. This is possible, due to rather rough surfaces of the aluminum plates by comparison with the glass plates used in commercial LC cells. The rather weaker and broader transmission resonances at zero volts may also reflect a lack of perfect alignment.

For intermediate voltages the situation is a little more complex. Now the director tends to homeotropic alignment at the center of the gap between two plates while remaining homogeneous at the boundaries. Thus the microwaves experience a distribution of refractive index across each cavity, the highest (guiding) index being at the center. However, because of the long wavelength of the microwaves, and the narrowness of the gaps relative to that wavelength, the microwave field distribution may be treated as quasiuniform.

The effective index for each mode is, then, to first order, the average calculated from the spatial profile of the director field. Continuum elastic theory¹⁴ is used to model the tilt angle, θ , distribution with the parameters of E7: ($\epsilon_{\parallel} = 19.50$, $\epsilon_{\perp} = 5.40$, $k_{11} = 1.15 \times 10^{-11}$ N, and $k_{33} = 1.46 \times 10^{-11}$ N). From this the effective local index is calculated using $n_{\text{eff}} = n_o n_e / (n_e^2 \cos^2 \theta + n_o^2 \sin^2 \theta)^{1/2}$, with $n_e = 1.800$ and $n_o = 1.647$. Finally, by integrating across the liquid crystal layer the average effective index is found as a function of applied field. This is shown as the solid line in Fig. 4. This is not a theoretical fit to the experimental data. It merely serves to confirm that the resonant mode shifts are in accord with the simple model of the low voltage induced reorientation of the LC.

In conclusion, a low-voltage-controlled, liquid-crystal-based wavelength selector for the microwave frequency range of 26.5–40.0 GHz has been realized. This comprises a zero-order metal slat grating structure in which the thin inter-slat cavities are filled with nematic liquid crystal. In these cavities coupled surface plasmons are excited which, for certain incident wavelengths, set up standing waves. These wavelengths are selectively transmitted. By varying the voltage applied to the slats, these resonant transmission frequencies may be adjusted. A simple model which treats the structure as a filled Fabry-Pérot fits the data obtained rather well. Combining this with an elastic continuum model for the response of the liquid-crystal director fully explains all the mode positions and their variation with voltage.

Serious exploitation of such devices is likely to need improvement in contrast by obtaining better alignment, perhaps by using more highly polished aluminum slats, and

probably less absorbing liquid crystals specifically designed for microwave work.

The authors would like to thank the Engineering and Physical Science Research Council and the UK Ministry of Defense for their financial assistance through the Joint Grant Scheme. Helpful discussions with Dr. C. R. Lawrence of the Defense Evaluation and Research Agency (Farnborough) are also appreciated.

- ¹K. C. Lim, J. D. Margerum, A. M. Lackner, L. J. Miller, E. Sherman, and W. H. Smith, Jr., *Liq. Cryst.* **14**, 327 (1993).
- ²K. C. Lim, J. D. Margerum, and A. M. Lackner, *Appl. Phys. Lett.* **62**, 1065 (1993).
- ³K. C. Lim, J. D. Margerum, A. M. Lackner, and E. Sherman, *Mol. Cryst. Liq. Cryst.* **302**, 187 (1997).
- ⁴F. Guerin, J. M. Chappe, P. Joffre, and D. Dolfi, *Jpn. J. Appl. Phys., Part 1* **36**, 4409 (1997).
- ⁵T. W. Ebbesen, H. J. Lezec, H. F. Ghaemi, T. Thio, and P. A. Wolff, *Nature (London)* **391**, 667 (1998).
- ⁶T. Thio, H. F. Ghaemi, H. J. Lezec, P. A. Wolff, and T. W. Ebbesen, *J. Opt. Soc. Am. B* **16**, 1743 (1999).
- ⁷T. J. Kim, T. Thio, T. W. Ebbesen, D. E. Grupp, and H. J. Lezec, *Opt. Lett.* **24**, 256 (1999).
- ⁸J. A. Porto, F. J. Garcia-Vidal, and J. B. Pendry, *Phys. Rev. Lett.* **83**, 2845 (1999).
- ⁹U. Schroter and D. Heitmann, *Phys. Rev. B* **58**, 15419 (1998).
- ¹⁰N. P. Wanstall, T. W. Preist, W. C. Tan, M. B. Sobnack, and J. R. Sambles, *J. Opt. Soc. Am. A* **15**, 2869 (1998).
- ¹¹M. B. Sobnack, W. C. Tan, N. P. Wanstall, T. W. Preist, and J. R. Sambles, *Phys. Rev. Lett.* **80**, 5667 (1998).
- ¹²H. E. Went, A. P. Hibbins, J. R. Sambles, C. R. Lawrence, and A. P. Crick, *Appl. Phys. Lett.* **77**, 2789 (2000).
- ¹³M. Born and E. Wolf, *Principles of Optics*, 7th ed. (Cambridge University Press, Cambridge, 1999).
- ¹⁴H. J. Deuling, *Mol. Cryst. Liq. Cryst.* **19**, 123 (1972).